Eurographics Workshop on Visual Computing for Biology and Medicine (2012)
T. Ropinski, A. Ynnerman, C. Botha, and J. B. T. M. Roerdink (Editors)

Lowest-Variance Streamlines for Filtering of 3D Ultrasound

Veronika Šoltészová[1] Linn Emilie Sævil Helljesen[2] Wolfgang Wein[3] Odd Helge Gilja[2] and Ivan Viola[1]

[1]University of Bergen, Norway
[2]National Centre for Ultrasound in Gastroenterology, Haukeland University Hospital, Norway
[3]Technical University of Munich, Germany

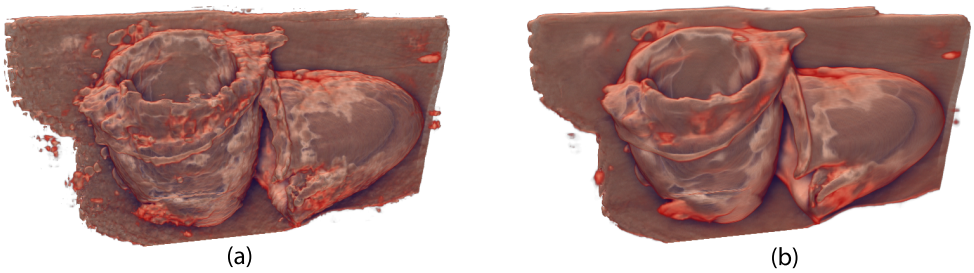

Figure 1: *Comparison of (a) a visualization of a raw 3D ultrasound scan of a phantom dataset and (b) a visualization of the same dataset filtered with the lowest-variance streamline method.*

Abstract

Ultrasound as an acoustic imaging modality suffers from various kinds of noise. The presence of noise especially hinders the 3D visualization of ultrasound data, both in terms of resolving the spatial occlusion of the signal by surrounding noise, and mental decoupling of the signal from noise. This paper presents a novel type of structure-preserving filter that has been specifically designed to eliminate the presence of speckle and random noise in 3D ultrasound datasets. This filter is based on a local distribution of variance for a given voxel. The lowest variance direction is assumed to be aligned with the direction of the structure. A streamline integration over the lowest-variance vector field defines the filtered output value. The new filter is compared to other popular filtering approaches and its superiority is documented on several use cases. A case study where a clinician was delineating vascular structures of the liver from 3D visualizations further demonstrates the benefits of our approach compared to the state of the art.

Categories and Subject Descriptors (according to ACM CCS): I.4.3 [Image processing and computer vision]: Enhancement—

1. Introduction

Medical ultrasound enjoys popularity as the most preferred imaging modality in a number of diagnosis and treatment scenarios [ØGG05]. This acoustic-reflectance based modality has valuable characteristics in terms of practical bedside usage and low price [GHW*03]. Most importantly, as a live modality, it has an unbeatable temporal resolution and its spatial resolution can be superior to standard 3D modalities, e.g., computed tomography and magnetic resonance imaging. Moreover, measuring acoustic phenomena with ultrasound can provide useful information about flow, elasticity, or strain of imaged tissue [GHH*02]. Very important for patient safety is that no ionizing radiation is associated with ultrasound examination, and its usage within mechanical-index limits is considered safe. Furthermore, by adding contrast agents using low mechanical index, new diagnostic and therapeutic possibilities have opened up [PG07, PG11].

The gravest disadvantage of ultrasound imaging is the

DOI: 10.2312/VCBM/VCBM12/041-048

high presence of various types of noise that impede the image interpretation. They have been intensively studied and can be categorized into two distinct categories: random and structured. Structured noise can be further categorized into subcategories such as acoustic scattering (speckle), shadowing, or dropout. With regard to 2D ultrasound images, most of these noise types can be distinguished by the sonographer with a substantial experience. Moreover, speckle noise is often considered as a useful source of information, and there are debates whether to keep speckle in diagnostic 2D-ultrasound imaging.

3D ultrasound visualization is very different from the 2D case, however. In 3D renderings, random and structured noise impede the visual reconstruction of imaged structures, occlude it, modify it, and are the origin of normal perturbation that becomes a dominant effect when calculating local illumination. Therefore, for 3D visualization the goal is to eliminate the noise entirely and give prominence to the signal. Noise removal filters, however, can potentially modify the signal up to such an extent that it is no longer diagnostically relevant. Finding a clear separation between signal and noise is not trivial, and cannot be handled by common linear and non-linear filters.

The scope of the presented work is a novel structure-preserving filtering approach that is based on a local variance distribution, and is designed specifically for the 3D ultrasound visualization pipeline. Figure 1 demonstrates the method on a phantom model of the myocardium [FLM11]. Unlike traditional filters, its operator mask is a curve that locally aligns to the structure. This eliminates structure thinning or removal of structural details, as is typical for other filter-types reviewed in Section 2. Details on algorithmic description of the new filter are provided in Section 3. The filtering is demonstrated on several ultrasound phantom and anatomical datasets in Section 4, and its structure-preserving behavior is evaluated in Section 5. Finally, the paper draws conclusions on conducted research in Section 6.

2. Related work

A large body of research has been devoted to preprocessing and data enhancement for ultrasound. Sakas et al. [SSG95] listed techniques with a good trade-off between loss of information and quality. A recent survey by Birkeland et al. [BSH*12] provides a concise overview over the ultrasound visualization pipeline, where several approaches include a pre-filtering step prior to rendering. In this section, we review only the most relevant works related to noise reduction in ultrasound.

The following works are performing enhancement based on local data homogeneity. Kuwahara et al. [KHEK76] described a filter which divides the neighborhood of a point P into blocks and the filtered value in P was the mean value of the most homogeneous block, i.e., block with lowest variance. Karaman et al. [KKB95] presented an adaptive filtering technique for speckle removal for B-mode ultrasound. Smoothing operators (mean or median) are applied in regions where the tissue is assumed homogeneous. These regions are obtained by region growing which is constrained only by statistical properties and the distance from the central pixel. Yanhui et al. [YCJY09] performed directional averaging based on 2D homogeneity. Pixels, which have their homogeneity above a certain threshold, remain unchanged. Other pixels are processed by their directional average filter. An edge detection is followed by directional filtering along the edge with the highest edge-value (vertical or horizontal). Farzana et al. [FTM*10] used a combination between the Euclidean distance between the origin pixel O and a neighborhood pixel J, and a homogeneity parameter of O. This parameter is obtained from blocks of O's neighborhood which have homogeneity above a certain threshold. Bilateral filters combine pixels based on their geometric closeness and photometric similarity [TM98]. Viola et al. [VKG03] presented hardware-based implementations of the median, bilateral filter, and the Kuwahara filter.

Statistical analysis of data has been facilitated for filtering and segmentation purposes in a number of works. Czerwinski et al. [CJO95] proposed an adaptation of a median filter to solve the problem of boundary-preserving speckle reduction in ultrasound. They took a set of short lines passing through the center of a square-shaped kernel. Along each line, they computed the median. Finally, they kept the largest median value for the pixel in the center of the kernel. In their follow up work, they described how lines can be detected in ultrasound images [CJO98]. They also discussed different methods for hypothesis testing that the actual line is going through the edge in the picture. Coupé et al. [CHKB09] adapted the nonlocal means filter [BCM05] based on Bayesian statistics. Instead of a simple distance weighting used in the original nonlocal means filter, they used the Pearson Distance between two random variables X and Y that is based on their correlation $1-\rho_{XY}$.

Statistical properties were also used for determining tissue similarity in general. Patel et al. [PHBG09] used statistical moments (variance in combination with mean) for segmentation of noisy datasets. They used statistical moments to determine similarity between tissues. Their approach could be adjusted for automatic design of the operator mask. Fattal and Lischinski [FL01] used a variational approach for opacity classification of 3D ultrasound datasets.

Several works pursued adaptive filter design. Chinrungrueng and Suvichakorn [CS00] employed polynomial surface fitting to the intensities. They reported results which were at least as good as results produced by a median filter but could be obtained for less computation time. Caan et al. [CKP*10] described an adaptive filtering kernel which depends on the space-variant level of noise and some similarity measures

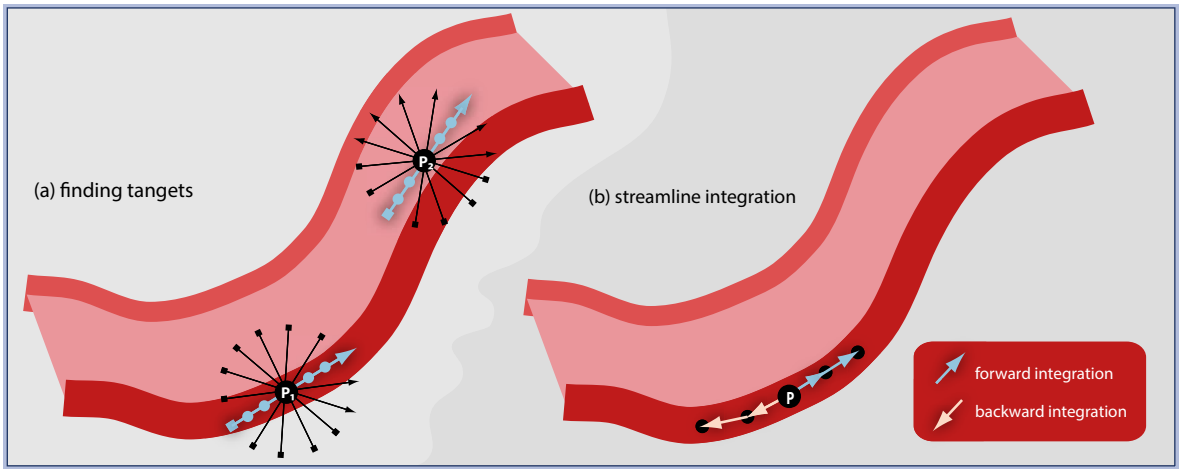

Figure 2: *Determination of the line segment n=3 with the lowest variance of intensities at two points P_1 and P_2 (a). Streamline integration seeded in point P (b). Forward integration is shown in blue and backward integration in pink.*

to the central pixel. The adaptation was done as a weighted Gaussian filtering where the weights were related to the similarity of the neighborhood tensors. Eom [Eom11] determined the shape and the orientation of the filter based on distance and angle maps, i.e., distance of a pixel to the nearest edge. The filter was then aligned to the edge tangent at the closest point of the closest detected edge.

Su and Seul proposed filtering with wavelets [SS01]. They replaced small wavelet coefficients by zero and kept or shrank other coefficients. Anisotropic diffusion is a frequently applied filtering method which smooths inside regions but not the edges itself [PM87]. The edges are defined by local gradients. Michailovich and Tannenbaum [MT06] conducted a study where they compared performances of three nonlinear filters: wavelet denoising, total variation filtering [ROF92] and anisotropic diffusion; and demonstrate their applicability for speckle removal in medical ultrasound.

This short review of filtering methods illustrates the large body of existing work that has addressed the problem of ultrasound denoising. Still, to the best of our knowledge, there is no work that took an approach similar to our lowest-variance streamline filtering, and is specifically designed to improve 3D ultrasound visualization. It is too preliminary to claim that our technique outperforms any other form of filtering. In this paper though, we have conducted first comparative steps and relate our work to a selection of the most frequently used structure-preserving and denoising approaches.

3. Filtering Method

Speckle noise in 3D ultrasound poses a challenge to volume visualization since it obstructs interpretation and identification of structures. To improve the quality of 3D rendering, it is desired to perform a speckle-removal procedure. In data processing for the medical domain, it is very important to preserve the boundaries of structures. This is a problem of many filtering techniques: even though the boundaries and edges are preserved, they move or change shape.

There have been attempts to preserve edges by using bilateral filters using weighted averaging taking into account the distance and intensity similarity between voxels. This approach is however sensitive to noise since the intensity similarity factor is based only on differences (local property of two points). Our approach pursues a different strategy. We are performing a selective averaging, but the selection which voxels will be taken into account is novel with respect to previous work. The filtering happens in two stages each of which can be parallelized:

1. **Determine the tangent direction** For each point P in the volume (a voxel in our context), select the direction which has the highest probability of all directions **x** to be tangent to a fictive surface going through P. The outcome of this stage is a 3D vector field.
2. **Integrate** For each point P, construct a short streamline seeded in P by integration of the vector field produced in the previous stage. The streamline defines the shape of the filtering operator mask.

With many speckle removal techniques available, our method is, to the best of our knowledge, the only technique which utilizes the principle of streamline integration to snap the filtering kernel to object boundaries. In this manner, we ensure after filtering, the boundaries have moved minimally and have preserved their intensity. In Sections 3.1 and 3.2, we describe each of the stages.

3.1. Local Direction of Lowest Variance

The ultrasound-inherent speckle noise poses a challenge to any local processing technique of this modality. When determining the tangent directions it is therefore necessary to evaluate a larger neighborhood, in order to find the direction of a boundary going through a voxel in noisy data. We are evaluating variance in patterns within a local neighborhood, since this is a robust measure used also in previous work for data classification [PHBG09].

We assume that values along a line segment entirely inside one tissue material will have lower variance of intensities than a line segment which is crossing several materials. To find the orientation of a line segment with lowest variance for every voxel, we proceed as follows. We align line segments centered in a point P to a discrete set of directions. These directions are obtained by rotating an initial line segment in the XY and XZ plane around P by an angle δ. This assures a minimal angular sampling rate of δ, in our implementation 5°.

Each line segment is defined by the position P and the direction vector **x**. Since both vectors **x** and -**x** could define the same line, we consistently select **x** with a positive y-coordinate. Then we calculate variance of the set of samples for each of the line segments. The direction $\mathbf{x}_{min}$ which corresponds to the line segment with the lowest variance will be copied to the output 3D vector field at the position of P. Formally, we define $\mathbf{x}_{min}$ as follows:

$$\mathbf{x}_{min} \mid \forall \mathbf{x}, \underset{k\in-n..n}{Var}\{f(P+k\Delta\mathbf{x})\} \geq \underset{k\in-n..n}{Var}\{f(P+k\Delta\mathbf{x}_{min})\}$$

where $Var\{.\}$ is the variance of a set of values, $f(P)$ is the voxel intensity at point P, Δ is a positive step size and n indicates how many samples are taken along the line segment in the positive and in the negative negative sense. In our approach, we used $n = 5$, where each $\Delta\mathbf{x}$ amounts to the size of a single voxel. The principle is shown in Figure 2a simplified in 2D. The $\mathbf{x}_{min}$ is shown in blue, all other line segments are shown in black.

3.2. Streamline Integration and Filtering

In the first stage, we obtained a 3D vector field where each vector represents the direction of the line segment with minimal variance. At this point, we continue with the construction of the operator mask for each voxel P separately. This procedure is similar to streamline integration with P being the seed point. See also the illustration in Figure 2b.

1. **Forward integration** constructs a part of the operator mask while integrating $\mathbf{x}_{min}$ from the underlying vector field. In Figure 2b, this part of integration is marked in blue.
2. **Backward integration** uses the inverted vector field, i.e., $-\mathbf{x}_{min}$ to construct the second part of the operator mask, in Figure 2b illustrated with pink.

Both the backward- and the forward-integration parts are employing the Runge-Kutta 4 integration scheme [Run95, Kut01]. In this way, we obtain $2m+1$ samples where m is the number of integration steps. The filtered value $\hat{f}(P)$ at point P is then determined as the arithmetic mean of these samples:

$$\hat{f}(P) = \frac{1}{2m+1}\sum_{i=-m}^{m} f(P_i)$$

With P_i being the i^{th} integration step of the streamline and $i > 0$ being the forward integration, $i = 0$ the seed point sample, and $i < 0$ backward integration. For the results presented in this paper, we used $m = 5$.

4. Results

We applied our technique to various 3D ultrasound and MRI data sets. Figure 1 shows the effect of the variance-streamline filtering applied to an ultrasound scan of a myocardium phantom. The phantom is manufactured from a synthetic polymer called PVA (polyvinyl alcohol) which has in crystallized form acoustic properties similar to the myocardium [FLM11]. We also filtered series of ultrasound volumes capturing a human cardiac cycle. Figure 3 shows additional pairwise comparisons of filtered and non filtered datasets: 3D cardiac volumes (pairs I and II), 3D liver ultrasound (III) and liver MRI (IV). The amount of speckle and noise significantly decreased, in particular in terms of smoothed myocardium walls and liver vessels. The noise level in the MRI dataset decreased significantly as well, while the edges remained clear.

In addition, we tested the technique by filtering the staircase artifacts on voxelized meshes. We applied several frequently using filtering approaches to the voxelized mesh: mean filter, Kuwahara filter, median filter. The mean filter creates fuzzy borders. The median filter and the Kuwahara filter preserve sharp edges, but do not remove the artifacts. Our method preserves borders and removes a large portion of the artifacts. The original mesh, as well as the voxelization and filtered datasets are compared in Figure 4.

In some cases, small features are of diagnostic importance, for example if a doctor is searching for aneurisms. We have not yet investigated the effect of our filtering on such structures, and therefore we cannot state that our filtering is safe to use in such cases.

We implemented this method as a preprocessing step in CUDA. While the second stage of the filtering process can be executed during rendering, the 3D vector field has to be

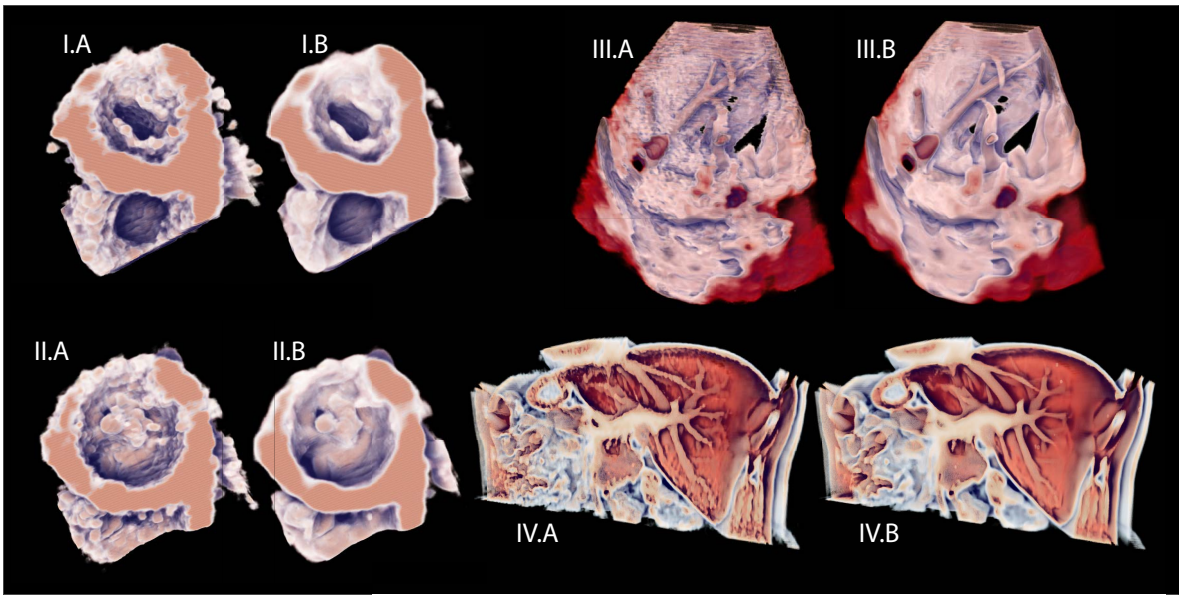

Figure 3: *Comparison of non-filtered and filtered datasets from medical ultrasound and MRI: I. and II. 3D cardiac ultrasound, III. 3D ultrasound of liver, and IV. MRI of liver.*

precomputed as thew computation takes approximately five seconds on modern graphics hardware for a volume of size 256^3.

5. Case Study

In data processing and in visualization, it is highly important to maintain structures so that they represent the anatomic situation as precisely as possible. An uncareful preprocessing could cause vessel thinning or sometimes even removing of thin branches. Vessels are, however, very important because, e.g., in the liver they are influencing preoperative planning decisions and are also useful for localizing pathologies. Anatomical partitioning of the liver is determined by the liver vessel tree [Cou57].

To assess the quality of our technique, especially its usability for filtering vessels in medical ultrasound datasets, we conducted a quantitative evaluation with a medical doctor specialized in gastroenterology. During the interpretation of ultrasound visualization, the clinician mentally "removes" the speckle and other kinds of noise. To compare the result of speckle removal from a visualization of non-filtered data, which is mentally filtered by a clinician, and filtered data with denoising filters, we conducted the following task.

We presented the clinician a series of visualizations of liver ultrasound without the pre-filtering. The visualizations were printed in an A4 format and put into an adhesive transparent foil. The medical doctor used a marker to outline the vessel tree in the liver. For each of three liver datasets, she received visualization of the original dataset and five pre-filtered versions using different techniques: median filter $3 \times 3 \times 3$, Kuwahara filter $3 \times 3 \times 3$, anisotropic diffusion with two distinct parameter settings, and our method. Concerning the anisotropic diffusion, it is difficult to automatically find a good parametrization (time step, κ, and the number of iterations) [Fri06]. Therefore, we produced results with a series of combinations and selected two best settings concerning structure preserving (diffusion I) and level of noise (diffusion II). Moreover, the same parameter setting might be suitable only for the dataset it was chosen for.

Our aim was to study, where the clinician observed the vessels in the original ultrasound dataset and compare these to the situation when this dataset is filtered with the most frequently used techniques and our technique. Figure 5 showcases our first test case including the original, i.e., the non-filtered dataset, and datasets filtered with five different techniques, including ours. Each visualization is juxtaposed to its corresponding line drawing made by the clinician. She used a green marker to draw vessels and a red marker to draw where she was not certain about the shape of the vessel wall. For the filtered datasets the clinician was instructed to solve the task of vessel delineation only using the information extracted from the visualization. Finally, for drawing over the non-filtered dataset, she was allowed to view the 3D rendering of the dataset in an interactive application to get better insights about the structures. Therefore we consider the vascular delineation in the non-filtered dataset as the one, which is best representing the structural arrange-

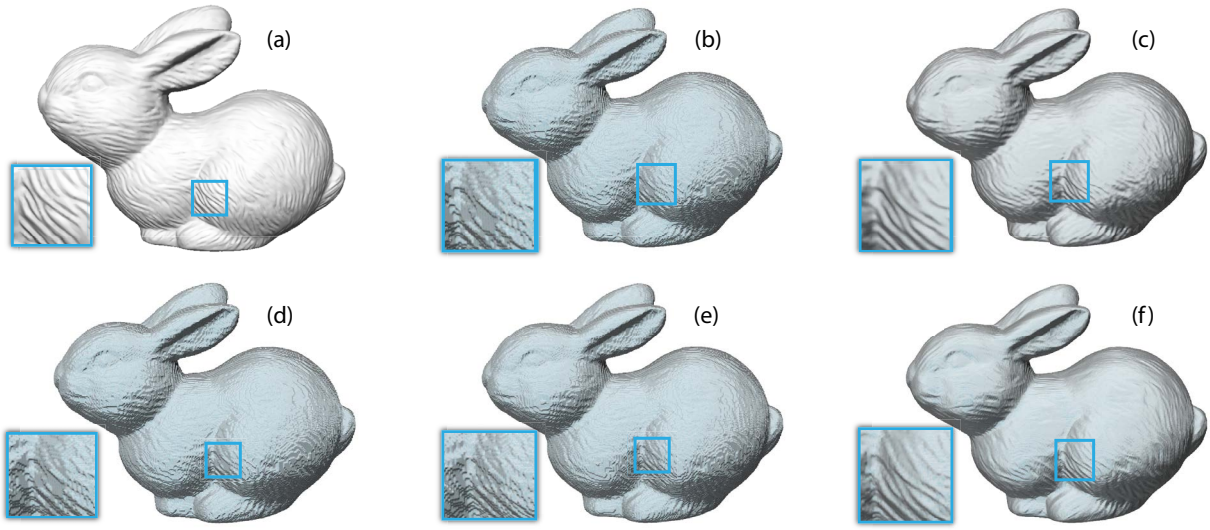

Figure 4: *Mesh representation of a laser scan of a bunny (a), voxelization of the mesh (b), filtered with mean filter* $3 \times 3 \times 3$ *(c), median filter* $3 \times 3 \times 3$ *(d) Kuwahara filter* $3 \times 3 \times 3$*, and our method* $n = 5$*,* $m = 5$*.*

ment. For benchmarking purposes the line drawing extracted from the filtered dataset is rated according to how close it is to the line drawing from the non-filtered dataset.

In total, we evaluated three different scenarios of human vessel tree in the liver I, II, and III. The first test cases including the corresponding line drawings is shown in Figure 5. Inspired the quantitative comparison method proposed by Cole et al. [CGL*08], we evaluated the similarity between line drawings extracted from the non-filtered dataset and filtered datasets. We will refer to the drawings based on filtered data "filtered drawings" and to line drawings based on original data as to "original drawings". To obtain a similarity measure, we first converted each line drawing to a binary image where 1 signifies line and 0 no line. Then we computed a distance field for each filtered drawing. To determine the similarity between an original drawing and a selected filtered drawing, we used element-wise multiplication of the distance field of the selected filtered drawing and the binary image of the original drawing. The sum of all values in the result image signifies the total summed error. In order to obtain a relative measure, we divided the summed error by the summed length of the corresponding filtered drawing. The summed length of a drawing is simply the number of pixels with value 1 in the binary mask. This relative measure is, in other words, an expected distance of each point on a filtered line drawing to the closest point on its corresponding original drawing. The relative distances are listed in Table 1. We can see that the variance streamline filtering has obtained the scores with the smallest relative distance to the original drawings (with one exception in scenario II).

Additionally, the clinician rated the techniques subjectively based on the following criteria:

- Are the borders clear or fuzzy? In general, it is difficult to define borders if they appear fuzzy.
- Are the borders jaggy? Finding and interpreting smooth borders is easier.
- Does the filtering mehod cause that parts of the vessel are "cut off", but a little further, it seems that the vessel continues? Interpretation is difficult in this case.

Based on the visualizations of data, she subjectively rated the filtering methods in the following order (best to worst): variance-streamline filtering (our method), median filtering, no filtering, diffusion I, diffusion II, and Kuwahara filtering. From the evaluation we can conclude that both in our quantitative evaluation method and in subjective preference the new variance-streamline filtering method was preferred over the other techniques.

Scene	Med	Kuwahara	Dif. I	Dif. II	VS
I	11.78	24.14	9.29	12.54	8.76
II	3.17	39.92	10.78	15.08	3.53
III	10.83	16.06	16.69	20.70	9.28

Table 1: *Relative distance between the illustration extracted from the non filtered dataset and filtered datasets using median (Med), Kuwahara, diffusion and variance-streamline (VS) filtering.*

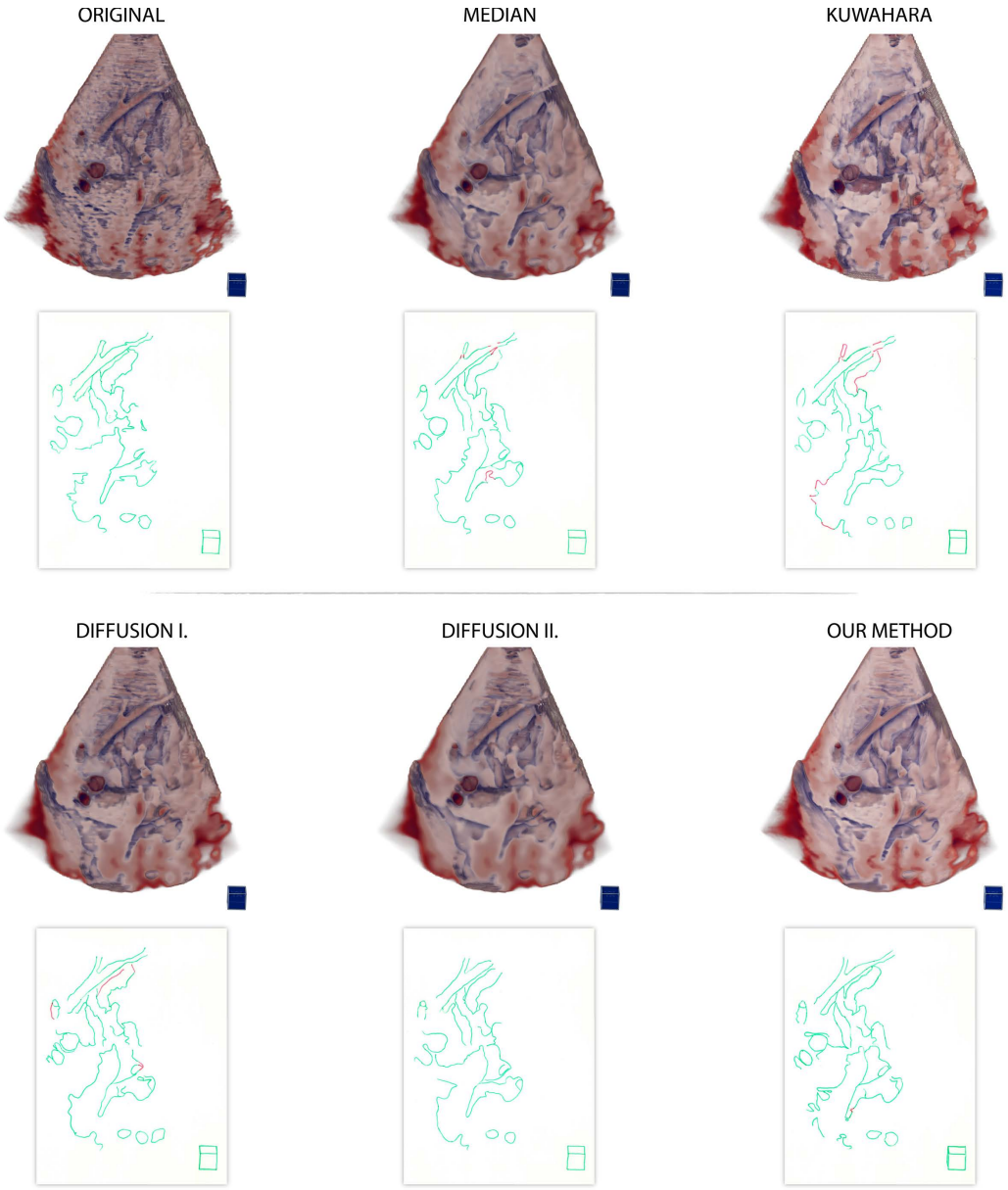

Figure 5: *Comparison of the visualizations of the original dataset, median filtering* $3 \times 3 \times 3$*, Kuwahara filtering* $3 \times 3 \times 3$*, diffusion I. (*Δ *= 3/44, 5 iterations,* κ *= 12), diffusion II. (*Δ *= 3/44, 7 iterations,* κ *= 14), and our method with n=5 and m=5. Below we showcase the corresponding line drawings made by the doctor. She used a green marker except of those lines where she was rather uncertain. The cube in the bottom right was used for registration of her drawings.*

6. Conclusions

We described a novel filtering approach which utilized the lowest variance direction to locally identify borders of structures, and based on this information, the operator mask is locally curved. This procedure is similar to streamline integration in a vector field. We showed its applicability especially on medical ultrasound, an imaging modality that is challenging 3D visualization due to its noisiness and speckle. In addition, we evaluated how the new filtering method affects understanding of structures in ultrasound. Based on the quantitative analysis and subjective judgment made by a clinician, we can conclude that our method preserves structures and at

the same time eliminates noise which makes the interpretation of the visualization easier.

References

[BCM05] BUADES A., COLL B., MOREL J.-M.: A non-local algorithm for image denoising. In *Proceedings of IEEE Computer Society Conference on Computer Vision and Pattern Recognition* (2005), vol. 2, pp. 60–65. 2

[BSH*12] BIRKELAND Å., SOLTÉSZOVÁ V., HÖNIGMANN D., GILJA O. H., BREKKE S., ROPINSKI T., VIOLA I.: The ultrasound visualization pipeline – a survey. *ArXive – e-prints* (2012). 2

[CGL*08] COLE F., GOLOVINSKIY A., LIMPAECHER H. S. B., FINKELSTEIN A., FUNKHOUSER T., RUSINKIEWICZ S.: Where do people draw lines? *ACM Transactions on Graphics 27*, 3 (2008). 6

[CHKB09] COUPÉ P., HELLIER P., KERVRANN C., BARILLOT C.: Nonlocal means-based speckle filtering for ultrasound images. *IEEE Transactions on Image Processing 52*, 5 (2009), 2221–2229. 2

[CJO95] CZERWINSKI R., JONES D., O'BRIEN JR. W.: Ultrasound speckle reduction by directional median filtering. In *Proceedings of the International Conference on Image Processing* (1995), vol. 1, pp. 358–361. 2

[CJO98] CZERWINSKI R., JONES D., O'BRIEN JR. W.: Line and boundary detection in speckle images. *IEEE Transactions on Image Processing 7*, 12 (1998), 1700–1714. 2

[CKP*10] CAAN M., KHEDOE G., POOT D., DEN DEKKER A., OLABARRIAGA S., , GRIMBERGEN K., VAN VLIET L., VOS F.: Adaptive noise filtering for accurate and precise diffusion estimation in fiber crossings. In *Proceedings of Medical Image Computing and Computer–Assisted Intervention* (2010), pp. 167–174. 2

[Cou57] COUINAUD C.: *Le foie. Études anatomiques et chirurgicales*. Masson et Cie, Paris, 1957. 5

[CS00] CHINRUNGRUENG C., SUVICHAKORN A.: Fast edge-preserving noise reduction for ultrasound images. In *IEEE Nuclear Science Symposium Conference Record* (2000), vol. 3, pp. 18/99–18/103. 2

[Eom11] EOM K. B.: Speckle reduction in ultrasound images using nonisotropic adaptive filtering. *Ultrasound in Medicine and Biology 37*, 10 (2011), 1677–1688. 3

[FL01] FATTAL R., LISCHINSKI D.: Variational classification for visualization of 3D ultrasound data. In *Proceedings of IEEE Visualization 2001* (2001), pp. 403–410. 2

[FLM11] FOSSÅ H., LUNDE P., MATRE K.: Ultrasound phantom for myocardium, 2011. 2, 4

[Fri06] FRITZ L.: Diffusion-based applications for interactive medical image segmentation. In *Proceedings of the Central European Seminar on Computer Graphics (CESCG)* (2006). 5

[FTM*10] FARZANA E., TANZID M., MOHSIN K., BHUIYAN M., HOSSAIN S.: Adaptive bilateral filtering for despeckling of medical ultrasound images. In *Proceedings of TENCON - IEEE Region 10 Conference* (2010), pp. 1728–1733. 2

[GHH*02] GILJA O. H., HEIMDAL A., HAUSKEN T., MATRE K., BERSTAD A., ØDEGAARD S.: Strain during gastric contractions can be measured using doppler ultrasonography. *Ultrasound in Medicine and Biology 28*, 14 (2002), 57–65. 1

[GHW*03] GILJA O. H., HAUSKEN T., WENDELBOE O., THIERLEY M., ØDEGAARD S.: Mobile ultrasound in a medical department – a pilot study. *Tidsskrift for den Norske Legeforening 19*, 27 (2003), 13–14. 1

[KHEK76] KUWAHARA M., HACHIMURA K., EIHO S., KINOSHITA M.: Processing of ri-angiocardiographic images. In *Digital processing of biomedical images*. Plenum Press, New York, USA, 1976, pp. 187–202. 2

[KKB95] KARAMAN M., KUTAY M., BOZDAGI G.: An adaptive speckle suppression filter for medical ultrasonic imaging. *IEEE Transactions on Medical Imaging 14*, 2 (1995), 283–292. 2

[Kut01] KUTTA M. W.: Beitrag zur näherungsweisen Integration totaler Differentialgleichungen. *Zeitschrift für Mathematik und Physik 46* (1901), 435–453. 4

[MT06] MICHAILOVICH O., TANNENBAUM A.: Despeckling of medical ultrasound images. *IEEE Transactions on Ultrasonics, Ferroelectrics, and Frequency Control 53*, 1 (2006), 64–78. 3

[ØGG05] ØDEGAARD S., GILJA O. H., GREGERSEN H.: *Basic and New Aspects of Gastrointestinal Ultrasonography*. Advanced Series in Biomechanics. World Scientific, 2005. 1

[PG07] POSTEMA M., GILJA O. H.: Ultrasound-directed drug delivery. *Current Pharmaceutical Biotechnology 8*, 6 (2007), 355–361. 1

[PG11] POSTEMA M., GILJA O. H.: Contrast-enhanced and targeted ultrasound. *World Journal on Gastroenterology 7*, 17 (2011), 28–41. 1

[PHBG09] PATEL D., HAIDACHER M., BALABANIAN J.-P., GRÖLLER M. E.: Moment curves. In *Proceedings of the IEEE Pacific Visualization Symposium 2009* (2009), pp. 201–208. 2, 4

[PM87] PERONA P., MALIK J.: Scale-space and edge detection using anisotropic diffusion. In *Proceedings of IEEE Computer Society Workshop on Computer Vision* (1987), pp. 16–22. 3

[ROF92] RUDIN L., OSHER S., FATEMI E.: Nonlinear total variation based noise removal algorithms. *Physica D 60* (1992), 259–268. 3

[Run95] RUNGE C.: Über die numerische Auflösung von Differentialgleichungen. *Mathematische Annale 46* (1895), 167–178. 4

[SS01] SU C., SEUL H.: A speckle reduction filter using wavelet-based methods for medical imaging application. In *Proceedings of the 23rd Annual International Conference of the IEEE Engineering in Medicine and Biology Society* (2001), vol. 3, pp. 2480–2483. 3

[SSG95] SAKAS G., SCHREYER L., GRIMM M.: Preprocessing and volume rendering of 3D ultrasonic data. *IEEE Computer Graphics and Applications 15*, 4 (1995), 47–54. 2

[TM98] TOMASI C., MANDUCHI R.: Bilateral filtering for gray and color images. In *Proceedings of the 6th conference on Computer Vision* (1998), pp. 839–846. 2

[VKG03] VIOLA I., KANITSAR A., GRÖLLER M. E.: Hardware-based nonlinear filtering and segmentation using high-level shading languages. In *Proceedings of IEEE Visualization* (2003), pp. 309–316. 2

[YCJY09] YANHUI G., CHENG H., JIAWEI T., YINGTAO Z.: A novel approach to speckle reduction in ultrasound imaging. *Ultrasound in Medicine and Biology 35*, 4 (2009), 628–640. 2